Nitrous and Pernitric Acids in and around Mexico City

David McCabe[1], Kathleen Spencer[1], John Crounse[1], Paul Wennberg[1], James Crawford[2], Jennifer Olson[2], Andrew Weinheimer[3], Lee Mauldin[3] and Christopher Cantrell[3]

[1]*California Institute of Technology, Pasadena, CA,* [2]*NASA Langley Research Center, Hampton, VA,* [3]*National Center for Atmospheric Research, Boulder, CO*

Abstract

Nitrous acid (HONO) and pernitric acid (PNA, HO_2NO_2) were measured from the NCAR C130 aircraft platform during the MILAGRO intensive in Mexico during the spring of 2006. Measurements were conducted *in-situ* using chemical ionization mass spectrometry. These observations provide a sensitive test of the coupled HOx / NOx chemistry in an urban environment. Measurements are presented along with comparison to box model calculations.

Motivation

- The goal of this research is to characterize the transport and transformation of gases on transcontinental/intercontinental scales and to assess their impacts on air quality and climate
- The outflow of Mexico City (a heavily polluted region, population ~20 million) has the potential to affect global atmospheric chemistry
- HONO and PNA, reservoirs of HO_x and NO_x, contribute to the transport of these radicals
- HO_x and NO_x radicals are of primary importance as they influence the production and degradation of O_3 and organic aerosol

Method

- NASA MILAGRO campaign in 2006 based in Mexico City
- NCAR C130 aircraft platform, altitude range of ~ 7 km
- Chemical ionization mass spectrometry (CIMS) using CF_3O^- as the reagent ion
- Highly sensitive (detection limits ≤ 50 pptv, 0.5 s collection) and quick time response (samples every ~ 5 s)
- Direct *in-situ* measurements of HONO and PNA
- Gas-phase measurement: rear-cut inlet rejects aerosol
- Fast flow through carefully selected inlet materials ensures minimal loss or sticking, even for difficult compounds such as HNO_3

Experiment

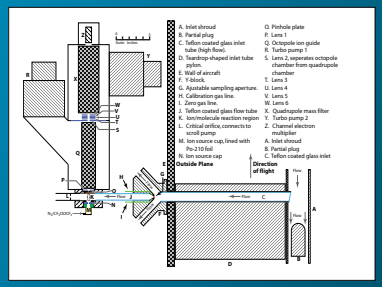

Figure 1: Schematic of CIMS instrument.

Ion Chemistry

HONO

$CF_3O^- + HONO \rightarrow HF \cdot ONO^-$ (*m/z* = 66) + CF_2O (fluoride transfer)

$CF_3O^- + HONO \rightarrow CF_3O^- \cdot HONO$ (*m/z* = 132) (cluster – *very insensitive for HONO, not used)*

PNA

$CF_3O^- + HO_2NO_2 \rightarrow HF \cdot OONO_2^-$ (*m/z* = 98) + CF_2O (fluoride transfer)

$CF_3O^- + HO_2NO_2 \rightarrow CF_3O^- \cdot HO_2NO_2$ (*m/z* = 164) (cluster)

HONO

- HONO is a direct source of OH and NO in polluted areas via photolysis and the major source of OH radicals in the early morning
- The major source of HONO at the surface is believed to be the heterogeneous reaction of NO_2 and H_2O on surfaces
- The daytime gas-phase source is thought to be dominated by the reaction of OH radicals with NO radicals
- The primary sink is photolysis

$OH + NO + M \rightarrow HONO + M$ (R1)

$HONO + h\nu\ (\lambda < 370\ nm) \rightarrow OH + NO$ (R2)

Observations

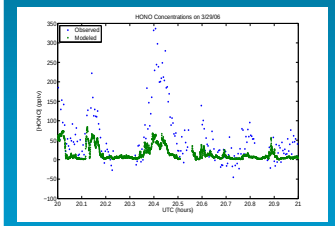

Figure 2. Observed and modeled HONO concentrations for representative flight 03/29/06

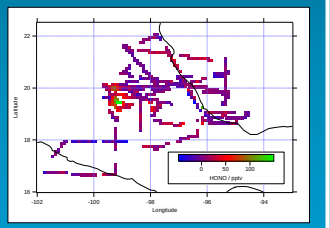

Figure 3. Map of measured HONO mixing ratios during 5 MILAGRO flights. Measurements are averaged for each grid point (0.1 x 0.1 degree)

Comparison with Box Model HONO

- Gas phase chemistry of HONO is simple
- Crawford, Olson *et al.* provided 1 second box-model data for HONO for comparison for selected times
- Model consistently under-predicts measured HONO in Mexico City metropolitan area plume

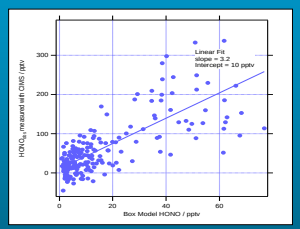

$$[HONO]_{SS} = \frac{k_1[OH][NO]}{J_2}$$

Figure 4. Box model calculation of HONO compared to observed HONO for a portion of flight 03/29/06

Summary

➢ Discrepancy between modeled and observed HONO

Possible Explanations:

a.) unknown interference at HONO mass (m/z = 66)

b.) OH is insufficiently constrained in the model

c.) There are additional sources of HONO beyond the reaction of OH with NO

PNA

- The source of PNA is the association reaction of HO_2 and NO_2
- Sinks include thermal decomposition, photolysis, and reaction of OH
- Under Mexico City conditions and altitudes sampled, thermal decomposition is the dominant loss process

$HO_2 + NO_2 + M \leftrightarrow HO_2NO_2 + M$ (R3)

$HO_2NO_2 + h\nu \rightarrow products$ (R4)

$HO_2NO_2 + OH \rightarrow H_2O + NO_2 + O_2$ (R5)

Observations

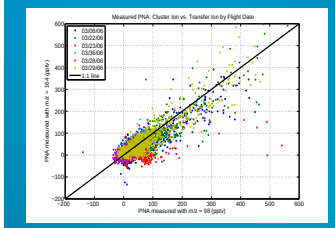

Figure 5. PNA is measured with two ions: products of fluoride transfer (*m/z* = 98) and clustering (*m/z* = 164), see Experimental section. Independent measurements of PNA from these two ions agree very well, indicating that these masses are selective to PNA. Final data uses both ions, under various concentrations of H_2O.

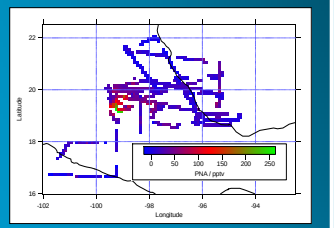

Figure 6. Map of measured PNA mixing ratios during 5 MILAGRO flights. Measurements are averaged for each grid point (0.1 x 0.1 degree).

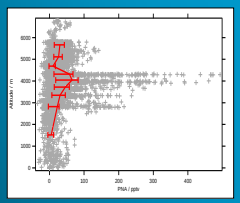

Figure 7. Vertical distribution of ~4700 0.5 s measurements of PNA during 5 flights during MILAGRO. Gray crosses are individual measurements; red line shows the average for each of 9 equally-sized bins. Error bars show the range of the middle two quartiles of each bin.

Increasing concentrations with altitude above 4500 m reflect the longer thermal lifetime of PNA. (Note that the flight patterns over Mexico City (alt. 2240 m) affects the altitude pattern of the data during MILAGRO.)

Comparison with Steady-State PNA

The dominant loss mechanism of PNA at these altitudes is thermal decomposition. In this simple regime, [PNA] can be modeled with the steady state expression:

$$[HO_2NO_2]_{ss} = \frac{k_3[HO_2][NO_2]}{k_{-3}}$$

Agreement between steady-state calculations of PNA and CIMS measurements is quite good, particularly when box model HO_2 is used

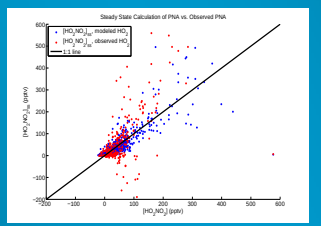

Figure 8. Box model calculation of PNA compared to measured PNA for 5 MILAGRO flights.

Summary

➢ Observed PNA is consistent with modeled values

➢ Observed PNA is better correlated with steady-state PNA using box model HO_2 than steady-state PNA using observed HO_2